Biogeosciences, 6, 807–817, 2009
www.biogeosciences.net/6/807/2009/

Biogeosciences

Comparing high resolution WRF-VPRM simulations and two global CO_2 transport models with coastal tower measurements of CO_2

R. Ahmadov[1], C. Gerbig[1], R. Kretschmer[1], S. Körner[1], C. Rödenbeck[1], P. Bousquet[2], and M. Ramonet[2]

[1]Max-Planck-Institute for Biogeochemistry, Hans-Knöll-Str. 10, 07745, Jena, Germany
[2]Laboratoire des Sciences du Climat et de l-Environnement, UMR CEA-CNRS 1572, 91191 Gif-sur-Yvette, France

Received: 29 September 2008 – Published in Biogeosciences Discuss.: 5 December 2008
Revised: 20 April 2009 – Accepted: 4 May 2009 – Published: 15 May 2009

Abstract. In order to better understand the effects that mesoscale transport has on atmospheric CO_2 distributions, we have used the atmospheric WRF model coupled to the diagnostic biospheric model VPRM, which provides high resolution biospheric CO_2 fluxes based on MODIS satellite indices. We have run WRF-VPRM for the period from 16 May to 15 June in 2005 covering the intensive period of the CERES experiment, using the CO_2 fields from the global model LMDZ for initialization and lateral boundary conditions. The comparison of modeled CO_2 concentration time series against observations at the Biscarosse tower and against output from two global models – LMDZ and TM3 – clearly reveals that WRF-VPRM can capture the measured CO_2 signal much better than the global models with lower resolution. Also the diurnal variability of the atmospheric CO_2 field caused by recirculation of nighttime respired CO_2 is simulated by WRF-VRPM reasonably well. Analysis of the nighttime data indicates that with high resolution modeling tools such as WRF-VPRM a large fraction of the time periods that are impossible to utilize in global models, can be used quantitatively and may help to constrain respiratory fluxes. The paper concludes that we need to utilize a high-resolution model such as WRF-VPRM to use continental observations of CO_2 concentration data with more spatial and temporal coverage and to link them to the global inversion models.

Correspondence to: R. Ahmadov
(rahmadov@bgc-jena.mpg.de)

1 Introduction

There is clear evidence in climate science that the continued increase of the atmospheric CO_2 content is caused by the anthropogenic emissions. However one of the scientific challenges is understanding the mechanisms responsible for removing anthropogenic CO_2 from the atmosphere. Observations demonstrate that about half of the emitted CO_2 is absorbed by biospheric sinks – the terrestrial biosphere and the ocean (Hansen et al., 2007). There are a number of essential questions related to the biogeochemical cycle of CO_2 to be solved by the scientific community. Modern coupled atmosphere-biosphere models suggest that, terrestrial ecosystems will provide a positive feedback in a warming world on a global scale (Heimann and Reichstein, 2008), which makes it essential to study the role and evolution of the giant natural carbon reservoirs. The leading questions are first of all the determination and also estimation of processes by which anthropogenic CO_2 is sequestered in the nature. It is also crucial to know the feedback mechanisms between the natural carbon cycle and the global climate system. The attempt to mitigate and also control the greenhouse gas emissions from different regions and countries requires estimating their carbon budget, which is a big challenge in the atmospheric sciences.

In order to answer the above mentioned questions, the atmospheric measurements of CO_2 from global networks are used in combination with inverse analysis to retrieve information on biosphere-atmosphere fluxes (Tans et al., 1990; Gurney et al., 2002). These approaches were operated based on annual and monthly atmospheric observations. Consequently the flux estimations of such inversion studies were very coarse in both time and space.

Since the estimation of the terrestrial biospheric sources and sinks is an essential task, there is a strong need to deploy continental observation sites. Historically, most of the

Published by Copernicus Publications on behalf of the European Geosciences Union.

continental sites were surface stations located on mountains and near coasts. In order to increase the representativeness of measurements sites, tall towers equipped with meteorological and greenhouse gas measurement devices were implemented to carry out CO_2 measurements at about 300 m above ground (Bakwin et al., 1995). Nevertheless, the location of any continental measurement site close to variable sources is often located in meteorologically complex areas: terrain-induced mesoscale phenomena such as sea-land (lake, river, forest, etc.) breezes, mountain-valley circulations, urban heat islands etc. make their representation in atmospheric models quite difficult.

Mesoscale effects generated by land surface heterogeneity and complex topography are usually on subgrid scales of current generation transport models used in inversions. In addition high resolution models are able to capture more accurately the front passing time and related effects at a site. An accurate simulation of front passing time at a measurement station is crucial since this may lead to strong jumps in CO_2 concentration (Wang et al., 2007). Further, in a model with coarse resolution complex boundary layer structures and thus vertical profiles of CO_2 over heterogeneous land cannot be adequately resolved. Mesoscale flows and mixing in the atmosphere are strongly correlated with short term variability of biospheric CO_2 fluxes, since they are both driven by the same mechanism, solar radiation. Hence inappropriate representation of the atmospheric transport on mesoscales may lead to significant biases in biospheric sources and sinks derived from inverse modeling. Thus all these effects can only be addressed with high resolution mesoscale simulations that include CO_2 fields in order to bridge the gap between measurements and inversion models.

The strong deterioration of CO_2 inversions due to transport model deficiencies are proven in some studies (Lin and Gerbig, 2005; Gerbig et al., 2008). In these studies uncertainties in advection and vertical mixing from ECMWF and ETA meteorological models are quantified and then linked to resulting errors in CO_2 inversions. The transport deficiencies become especially critical when trying to invert high space/time resolution of fluxes as compared to monthly fluxes on large regions for which data limitation is probably larger (Gurney et al., 2002). A comprehensive validation of different global (TM3, LMDZ) and regional (HANK, DEHM, REMO) offline transport models were done by (Geels et al., 2007) for several European tall towers and mountain stations. The intercomparison study revealed the remarkable improvement of the CO_2 concentration simulation by regional models with horizontal resolutions down to 50 km compared to the coarser global models. The conclusions made by Geels et al. (2007) impose severe limitations on the usability of continental CO_2 concentration data from short towers and mountain stations in inversions. Moreover one may also add coastal stations to the "difficult sites" list (Riley et al., 2005). As a result, the CO_2 inversions performed by the TransCom 3 inversion community down-weighted continental observations, assuming that the data contained too much "noise" (Gurney et al., 2004; Wang et al., 2007).

Another problem is the requirement of strict temporal data selection in inversions. Global CO_2 inversions usually use only afternoon hourly or even averaged values. Nighttime data or measurements taken during morning and evening hours are not used for most of the continental sites. Some of the inversion studies involve further filtering for day to day variability of CO_2 observation data to remove the "noise". Such filtering leads to losing the information about diurnal cycle of biospheric signals, which contains information on biospheric processes – respiration and photosynthesis, where for instance using nighttime data would make possible to constrain respiration fluxes. Thus it would be an obvious gain to use the full time series of continuous data for the inversion rather than only afternoon values. Using high-frequency concentration data would also be very useful for regional scale inversions which also could assist to close the gap between top-down and bottom-up estimations (Law et al., 2002).

As pointed out by Gerbig et al. (2009) there are several ways to mitigate the shortcomings of current inversion systems associated with uncertainties in transport representation of meteorological fields used for global inversion models. One of the promising solutions would be to apply transport models which better reproduce these processes. There are few studies addressing this problem by involving high-resolution atmosphere-biosphere models. Several mesoscale modeling systems are currently used to simulate mesoscale variations of CO_2 concentration in the atmosphere (e.g. Denning et al., 2003; van der Molen and Dolman, 2007; Sarrat et al., 2007; Ahmadov et al., 2007). In these studies mesoscale meteorological models in combination with biospheric models were used to perform forward simulations of CO_2. The studies show how strongly mesoscale flows initiated by complex terrain and by the land-water contrast could lead to remarkable gradients in atmospheric CO_2 fields. Such mesoscale model validations are also valuable since their meteorological fields can be used in regional inversions (Lauvaux et al., 2008).

This paper discusses the advantages of using very high-resolution mesoscale simulations for CO_2 transport versus two global CO_2 transport models in case of a coastal concentration measurement station – Biscarosse tower. The main goal of the paper is to address the deficiencies of the coarse resolution transport models in representing CO_2 point measurements which we have to take into account in the inversions targeted to estimate CO_2 fluxes. In addition the paper assesses the possibility of using hourly concentration data including nighttime in inversions by involving a mesoscale model. This work extends our previous study by Ahmadov et al. (2007), which compared WRF-VPRM simulations to aircraft data for a short time period, to a much longer simulation time period and a focus on one tower site.

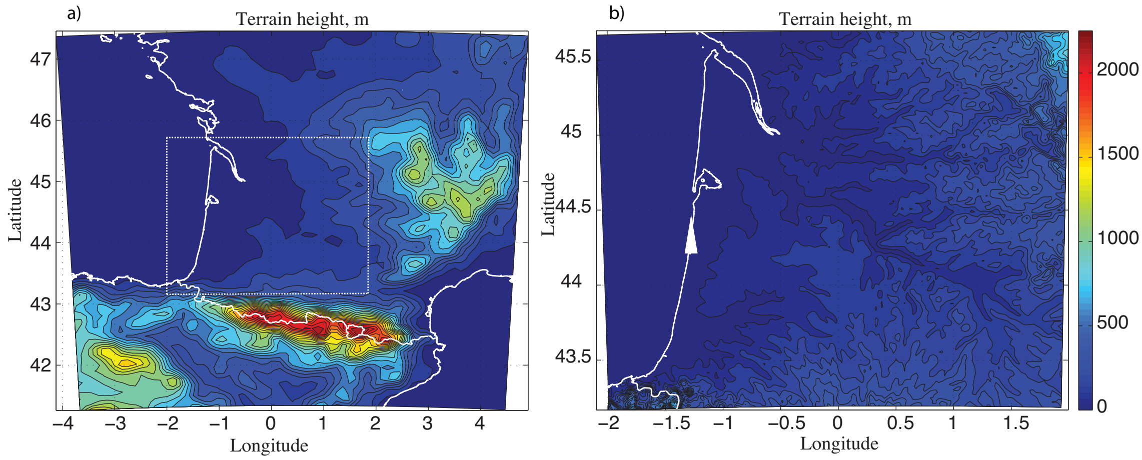

Fig. 1. Topography of the WRF domains – **(a)** the outer grid with 10 km resolution, the white box depicts boundaries of the inner domain, and **(b)** the inner grid with 2 km resolution, the white triangle indicates the Biscarosse tower location.

In Sect. 2 we describe the model setup. Section 3 introduces the observation campaign and the measurements. Section 4 presents a comparison of WRF-VPRM modeling results, global models and the observations. Finally, Sect. 5 summarizes the paper and discusses advantages and perspectives of using the WRF-VPRM modeling system for assimilating CO_2 concentration data from continental sites.

2 Configuration of the models

We set up and ran the Weather Research and Forecasting (WRF) model (http://wrf-model.org) at 10 and 2 km resolution on two nested grids (see Fig. 1a, b) over a domain that encompasses the area of the measurement campaign described in Sect. 3. The model was run in the two-way nested mode. In the two-way nest integration, the outer domain with 10 km (Fig. 1a) resolution provides the inner one (Fig. 1b) with lateral boundary conditions for the meteorological and CO_2 fields at every time step, simultaneously the 2 km grid solution replaces the 10 km grid solution for the points that lie inside the inner domain.

We coupled the diagnostic biospheric model Vegetation Photosynthesis and Respiration Model (VPRM) (Mahadevan et al., 2008) to WRF as a module. A detailed description of the WRF-VPRM modeling system can be found in (Ahmadov et al., 2007), here we provide only a brief overview. The VPRM model produces biospheric CO_2 fluxes in order to perform CO_2 tracer transport by WRF. The model uses MODIS (http://modis.gsfc.nasa.gov) satellite indices – enhanced vegetation index (EVI) and land surface water index (LSWI) obtained in 500 m spatial resolution with 8 days frequency. VPRM uses eight land-use classes with different parameters constraining CO_2 uptake and respiration fluxes. These parameters were optimized by using CO_2 flux measurements at few land-use classes located in the modeling domain. Furthermore the model used air temperature and radiation fields from the WRF model. For the VPRM model a high-resolution land cover map – SYNMAP (Jung et al., 2006) was used. A special preprocessing tool was used to preprocess land-use data and MODIS indices to map on a WRF grid. The preprocessing tool and the WRF-VPRM code are available freely to users upon request.

Anthropogenic CO_2 fluxes were taken from the 10 km resolution European anthropogenic emission inventory (updated in October, 2005) developed by the Institute of Economics and the Rational Use of Energy (IER), University of Stuttgart (http://carboeurope.ier.uni-stuttgart.de/). Lateral boundary conditions (LBCs) and initial conditions (ICs) for CO_2 concentration fields were taken from the global zoomed CO_2 transport model – LMDZ (Hourdin and Armengaud, 1999; Peylin et al., 2005) with a horizontal resolution of $0.83° \times 1.25°$ (latitude×longitude) over Europe, 28 vertical levels up to the tropopause, and half hourly time resolution (hourly for outputs) for physical processes (3 min for dynamical processes). The model is nudged to the ECMWF (http://www.ecmwf.int/) global model data to perform the meteorological transport. The LMDZ CO_2 fields used here are based on forward runs using CO_2 fluxes generated by the ecophysiological model – SiB2 (Sellers et al., 1996) together with fossil and ocean fluxes. Further an offset (376 ppm) was added to the model output to fit some of the European measurement sites.

All necessary meteorological data for initial and lateral boundary conditions, sea surface temperature and soil initialization fields of WRF were taken from the ECMWF analysis data (http://www.ecmwf.int/) with ≈35 km horizontal resolution and 6 hourly intervals.

The WRF-VPRM model was validated against a number of meteorological and tracer observations, both ground and aircraft based (Sarrat et al., 2007; Ahmadov et al., 2007;

Table 1. Parameters and physics options used in the WRF model.

Vertical coordinates	Terrain-following hydrostatic pressure vertical coordinate
Basic equations	Non-hydrostatic, compressible
Grid type	Arakawa-C grid
Time integration	3rd order Runge-Kutta split-explicit
Spatial integration	3rd and 5th order differencing for vertical and horizontal advection respectively; both for momentum and scalars
Domain configuration	2 domains with resolution – 10 and 2 km for outer and inner domains respectively; size 690×690 km and 320×280 km; 51 vertical levels for both domains up to 150 mb, where first 20 layers are located below 2 km height from the ground
Time step	60 and 12 s for outer and inner domains, respectively
Physics schemes	Radiation – Rapid Radiative Transfer Model Longwave and Dudhia shortwave Microphysics – WRF Single-Moment 3-class simple ice scheme Cumulus-Kain-Fritsch scheme (only for the coarse domain) PBL – Yonsei Univeristy; Surface layer – Monin-Obukhov Land-surface – Noah

Macatangay et al., 2008). One improvement of WRF-VPRM in the current study is the online coupling of VPRM to WRF, so that WRF produced air temperature at 2 m (T2) and shortwave downward radiation (SWDOWN) were used in VPRM to calculate CO_2 fluxes which were then provided to WRF at each integration time step. Table 1 shows the WRF model physics and grid options for these runs. In WRF-VPRM we used several concentration fields, so called "tagged tracers", for CO_2 corresponding to the different origins: 1) total CO_2 concentration (which can be measured) that combines CO_2 fields from anthropogenic and biospheric sources and also coming from the outside of the simulation domain; 2) global CO_2 that does not include any uptake or emission fluxes within the WRF domains, which participates only in transport; 3) anthropogenic CO_2; 4) respiration and 5) photosynthesis signals. The last three "tagged" tracers include only the corresponding surface fluxes. They use zero inflow and zero-gradient outflow lateral boundary conditions, zero fields for initial conditions. The first two "tagged" tracers use CO_2 concentration fields from a global model in inflow and zero-gradient conditions on outflow, global fields for ICs. The "tagged" tracers allow us to separate the global CO_2 signal from the regional one, and to determine the contribution of the different fluxes to the total CO_2 signal.

All anthropogenic and biospheric fluxes were added at each simulation time step to the CO_2 field in the lowest vertical level of the WRF grids. We ran WRF-VPRM for one month time period – from 16 May to 15 June, 2005. Here only simulation results from the high-resolution (2 km) inner nest are presented.

Another model involved in this study is the TM3 global model (Rödenbeck et al., 2003) with a horizontal resolution of $4^\circ \times 5^\circ$ (latitude×longitude), 19 vertical levels up to the tropopause, and hourly time resolution (using instantaneous concentrations every 3 h for output). It uses 6-hourly NCEP data as meteorological input. The purpose of adding this model to the comparison is to get an insight into how increasing resolution improves the simulation of CO_2 variability. The TM3 model results are based on a global inversion using atmospheric CO_2 concentration measurements. BIOME-BGC (Trusilova and Churkina, 2008) was used to generate CO_2 fluxes from the terrestrial biosphere as a prior for the TM3 inversion. It should be noted that the TM3 model did not use the Biscarosse site in the optimization of the surface fluxes.

3 CERES campaign

Within the CarboEurope Integrated Project (http://www.carboeurope.org/), the first intensive observation campaign of CERES (the CarboEurope Regional Experiment Strategy) was performed in the Les Landes area, South-West France, during May–June 2005 (Dolman et al., 2006). The experimental domain covers an area of about 250 km×150 km in southwest France (Fig. 1b). The region consists of different land-use classes such as ocean, forest, croplands, vineyards, rivers and urban areas. The Pyrenees Mountains and the Massif Central are located to the south and eastern part of the domain, respectively. There are two large cities located close in the southeastern (Toulouse) and northwestern

(Bordeaux) edges of the domain. According to the local climatology the dominant winds should be either from the west or the east; therefore, the experiment was designed to observe modification of the CO_2 concentration profiles by the land as the air mass progressed east- or westward (Dolman et al., 2006).

During the campaign CO_2 concentration measurements were carried out by several surface stations and also by aircraft (Ahmadov et al., 2007). Several CO_2 eddy-flux and surface meteorological stations were also deployed during the experimental campaign. A high-precision CO_2 instrument (CARIBOU, with an accuracy of 0.1 ppm) was installed and operated on a 40-m high tower near Biscarosse (44.38° N, 1.23° W) (Fig. 1b) (Dolman et al., 2006). The measurement site is located about 2 km from the sea shore, and about 120 m above sea level. In addition we involved data from the meteorological station BISCAROSSE/PARENTIS located in the vicinity (44.43° N, 1.25° W) of the tower to aid interpreting CO_2 measurements, given that there were no meteorological measurements made at the tower itself. During the campaign other surface CO_2 stations (e.g. in Marmande and La Cape Sud areas) were operated, however those measurements were taken very close to the ground. Therefore we have involved only the Biscarosse site in this study.

The Biscarosse site is located at 2 km distance from the coast (Fig. 1b), thus the small area of the land biosphere between the tower and the ocean is not expected to change the marine air masses' CO_2 content significantly while the air is transported to the site by westerlies. Thus the tower detects marine air masses, with measurement periods that have large scale representativeness, but also air masses coming from inland with influences from the terrestrial biosphere and anthropogenic emissions. We chose this site for the current study assuming that the Biscarosse data might be used in future inversion studies (Lauvaux et al., 2008).

4 Results and discussion

Here we present the results for WRF-VPRM simulations for the Biscarosse site and the nearby weather station. Figure 2 exhibits a comparison of air temperature (T2) simulated by WRF and observed by the meteorological station. This plot gives insight into weather evolution over the period as well as the model performance for the important meteorological variable (T2), which also drives biospheric CO_2 fluxes. After a cold front passed on 17 May the weather became warmer, with sunny conditions on the following days. The south-westerly flows were bringing warm air masses to the region and thereby keeping the air temperature very high during 25–27 May. The fair weather was followed by synoptic perturbations and colder temperatures next days, except 1–2 June. On 8 June again anticyclonic conditions started prevailing and persisted until 12 June. Later the weather became cloudy and rainy over France by westerly flows pushed by a cyclone. The comparison reveals that the high-resolution model is able to accurately predict temperature variations with only a slight cold bias.

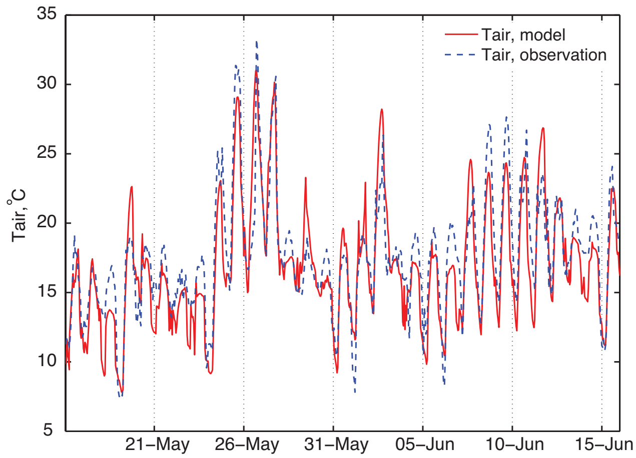

Fig. 2. Comparison of air temperature at 2 m between WRF simulated and measured one at the meteorological station – Biscarrosse Parentis. The statistics: r^2=0.77, average bias is −0.74°C, RMSE=2.14°C.

Figure 3a, b and c shows hourly CO_2 concentration measurements at the Biscarosse tower during one month together with simulated CO_2 from the global models TM3 and LMDZ, and from the mesoscale model WRF-VPRM. The figure shows how the models perform in capturing day to day variability of the concentration. Figure 3c shows that the WRF-VPRM model can capture much more variability in the observed time series than the two global models. Also the signal's amplitude of the signal is captured reasonably well for both daytime minimum and nighttime maximum by WRF-VPRM in many cases. Unlike the global models, WRF-VPRM is able to simulate the second maximum of CO_2 concentration in daytime which appeared due to the front passage or sea breeze in some days, e.g. during the 20, 26 and 27 May (Fig. 2).

The TM3 model shows some bias and less correlation with the observed data compared to LMDZ, which is as we argue due to its coarser resolution. For example, due to the gridcell size of several hundred kilometers within TM3 it is impossible to represent a coastal station correctly by the model under all flow conditions. The grid box comprising the Biscarosse tower is fully located over land in TM3, therefore the land influence is significantly overestimated, leading to stronger uptake as compared to the observations. It is worthy to note that TM3 and LMDZ have comparable performances when used with comparable resolution (Law et al., 2008).

LMDZ captures the observed daytime minimum and nighttime maximum in CO_2 concentrations with some discrepancy, while the average signal is captured quite well. Since the LMDZ model still has a relatively coarse horizontal

Table 2. Statistics of the comparison between measured and simulated CO_2 from the models for different cases – hourly, afternoon and nighttime averaged; R^2 – the square of the correlation coefficient, Bias- the mean bias, RMSE – root mean square error is the standard deviation of the differences between the models and the observations; Mean(std_{obs}) – the averaged standard deviation of the high-frequency CO_2 measurements from their hourly means.

Time	Model	R^2	Bias, ppm	RMSE, ppm	Mean(std_{obs}), ppm
Hourly	TM3	0.16	−3.87	5.09	0.58
	LMDZ	0.29	0.11	4.66	
	WRF-VPRM	0.59	0.67	4.26	
Afternoon Averaged	TM3	0.06	−2.49	3.67	0.35
	LMDZ	0.18	0.95	3.28	
	WRF-VPRM	0.52	−0.27	3.42	
Nighttime Averaged	TM3	0.02	−6.76	6.68	1.05
	LMDZ	0.22	−1.91	6.1	
	WRF-VPRM	0.58	0.95	4.95	

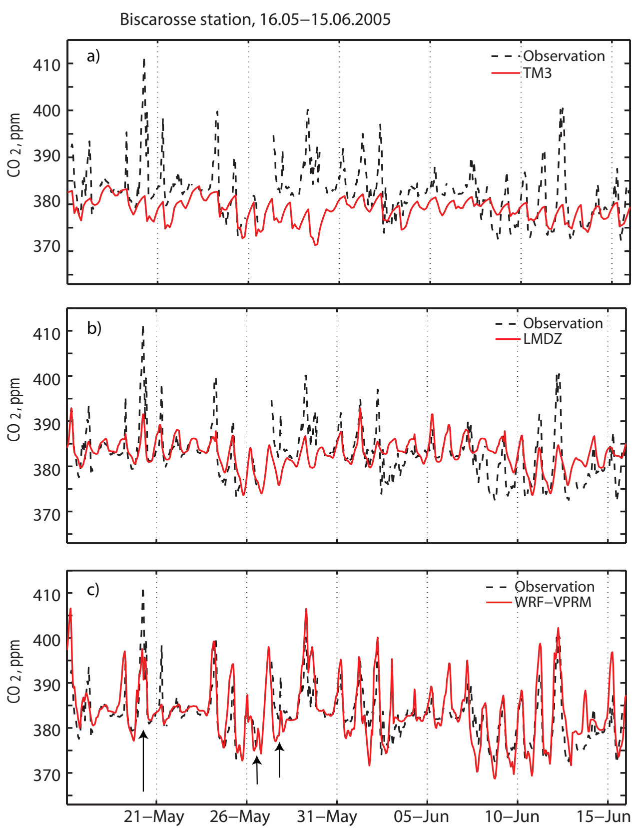

Fig. 3. CO_2 concentration time series from the Biscarosse tower and the models – **(a)** TM3, **(b)** LMDZ, **(c)** WRF-VPRM, the black arrows point different days: 20, 26 and 27 May.

resolution, it cannot accurately resolve subdiurnal variability in CO_2 concentration associated with atmospheric transport and mixing processes near the coastline.

The relevant statistics for the model-data comparisons can be found in Table 2, where also the mean standard deviation within the measurement periods of one hour is presented. The high root mean square error (RMSE) in the model-measurement comparison is partially caused by averaging the measurements over each hour, while using instantaneous values in the models. Averaging in the observation data is necessary to minimize the effects of eddies and other small scale effects that are not resolved by any of the models. Interestingly, the variability of CO_2 within an hour (last column of Table 2) is a factor of three smaller during day than during night, most probably due to stronger and deeper vertical mixing.

The numbers in Table 2 show that WRF-VPRM exhibits much more correlation compared to the global models. The main reason for such agreement is a better representation of the transport, especially mesoscale flows and vertical mixing in the 2 km resolution WRF-VPRM runs. In addition, the more accurate representation of the fine-scale variability in the surface CO_2 fluxes by VPRM, especially in the site's near-field, improves the CO_2 simulation as compared to the coarser global models. Although the average bias in LMDZ against hourly observation data is smaller, its deviation from the measurements (RMSE) is greater than in WRF. The existing discrepancy between the WRF-VPRM model and the measurements is caused by several reasons – uncertainties in CO_2 fluxes simulated by VPRM, initial and boundary conditions of CO_2 from LMDZ model, also uncertainties in transport and mixing within WRF. It should be noted that VPRM fluxes are based on a simple diagnostic model (Mahadevan et al., 2008). The model was validated against flux data and demonstrated its strong predictive ability for Net Ecosystem Exchange from hourly to monthly timescales (Mahadevan et al., 2008). Yet, the quality of VPRM fluxes would undoubtedly benefit from an optimization against atmospheric concentration measurements, while we only optimized the VPRM parameters against flux data from a few sites operated during the campaign (Ahmadov et al., 2007). VPRM is able to mimic the spatial and temporal distribution of surface fluxes by using high resolution satellite indices, land-use map and high spatiotemporal resolution meteorological fields from WRF. This approach is sufficient to determine the influence of main transport and mixing capabilities of the model on the CO_2 distribution.

In order to make clearer the contribution of different sources to the CO_2 concentration at the measurement location, we present hourly time series of the different "tagged" tracers from the WRF-VPRM model (Fig. 4). There is release of CO_2 by biosphere and accumulation of anthropogenic CO_2 in the shallow nighttime boundary layer. During some nights, for instance on 20 May there is an evident enhancement of both the biospheric and anthropogenic CO_2 fields since the tower detects inland respired CO_2 and also emission from power plants and other anthropogenic sources, but respired CO_2 largely dominates in amplitude. The analyzed time series reveal that in the CERES region during the summer season the biospheric CO_2 fluxes are dominant compared to the anthropogenic emissions, therefore we may neglect the anthropogenic component in further interpretations of the observations.

During persistent strong westerly winds (e.g. 21–23 May, 2005) both the biospheric and the anthropogenic CO_2 concentration at the site become negligible. In such instances the global CO_2 tracer plays the main role in contributing to the measured signal. During June the overall CO_2 uptake signals are stronger than during May, the first part of the simulation period. This behavior is caused by phenological changes associated with the intensifying growing season. Some of the large cropland areas in the region become strong CO_2 sinks in June as shown by Ahmadov et al. (2007).

A recirculation of respired nighttime CO_2 fields, for which the term "3-D rectifier effect" was established (Riley et al., 2005; Pérez-Landa et al., 2007; Ahmadov et al., 2007) is demonstrated for the case 20 May, 2005 (Fig. 5). During this day a south-westerly flow brought warm air masses over France. The weather was warm (Fig. 2) and sunny, with only some high clouds and weak westerly winds observed near the surface. It is obvious that this condition favors the formation of sea-land breeze, which enhances the westerly wind component of the surface wind towards afternoon. It is noteworthy that during this night the highest CO_2 signal of the May–June period at the Biscarosse tower was registered, with an enhancement of about 30 ppm compared to the afternoon values (Fig. 3a).

As Fig. 5a shows, WRF-VPRM underestimates this signal by about 10 ppm during the early morning when the nocturnal boundary layer is enriched with respired CO_2 advected from the inland by weak easterly winds (Fig. 5b). The un-

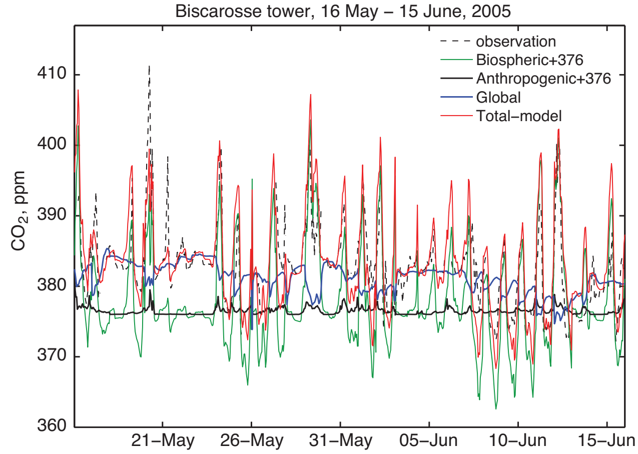

Fig. 4. Time series of the different tagged tracers at the tower site from the WRF-VPRM model.

derestimation might be related to overestimation of the easterly wind in WRF during that night when comparing to the measurements at the nearby weather station (Fig. 5c). There was stagnation in the air in early morning caused by convergence of westerly wind and land breeze. During this time the tower detected only respired CO_2 from the ground beneath. Since WRF could not well capture this case occurring around 05:00 UTC (07:00 local time), it failed also to resolve the huge respired CO_2 concentration by that time (see the "respired CO_2" tagged tracer time series in Fig. 5a). It is interesting to see that WRF-VPRM captures the minimum in CO_2 concentration at around 08:00 UTC (although 2 h earlier), associated with the change in wind through southerly at the onset of the sea breeze (Fig. 5b). Close to 10:00 UTC the strengthening and reversing wind flow becomes more westerly and brings a large plume of CO_2 respired during the previous night. Therefore we see a second strong maximum near 10:00 UTC in the measurement, but again a bit earlier in WRF-VPRM (Fig. 5a), since the wind rotation is faster in the model. After a few hours the westerly winds start bringing marine air masses with lower constant CO_2 concentration until the next day. The model captured this very well, indicating that the lateral boundary condition from the LMDZ model is appropriate. TM3 and LMDZ both show a smoothed diurnal cycle of CO_2 without a second maximum during this day due to coarse resolution.

In cases of strong synoptic disturbance the diurnal CO_2 signal at the site looks very different. For instance, on the 18 May, 2005 after the crossing of a cold front during the previous day, the wind shifted to north-west over the western part of France, colder and drier air moved into the country (Fig. 2). During this day the diurnal CO_2 concentration variation measured at the Biscarosse tower was less than 5 ppm (Fig. 3a). These are ocean air masses which are not affected by diurnal CO_2 fluxes as on the continent. This case was well simulated by all the models.

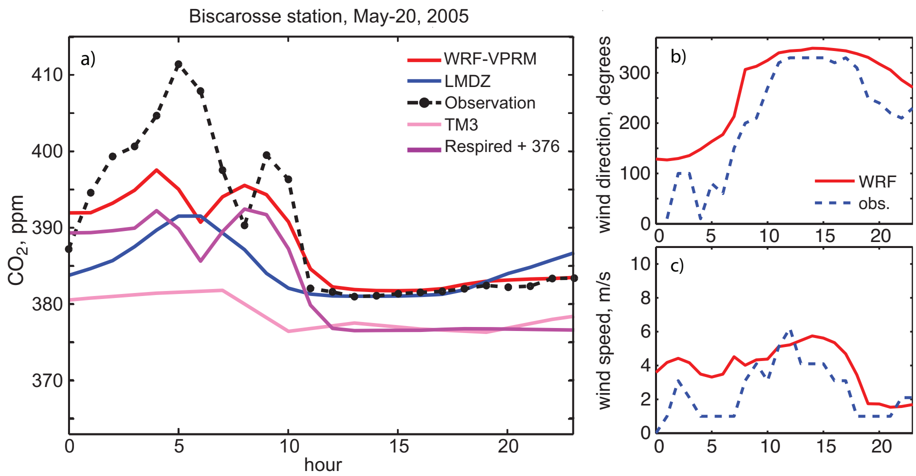

Fig. 5. (a) CO_2 concentrations from the models versus the observation for the 20 May, and respired tagged CO_2 tracer from WRF-VPRM; **(b)** wind direction and **(c)** wind speed comparison on that day at the nearby meteorological station; the time is given in UTC.

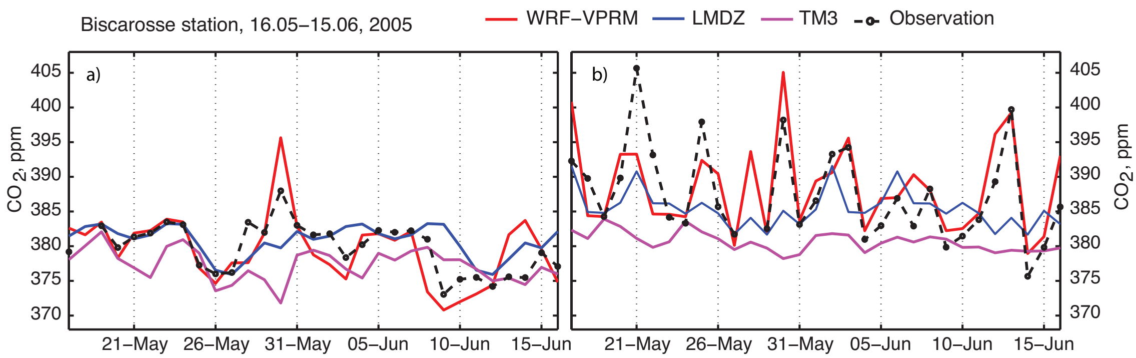

Fig. 6. Comparison of measured CO_2 concentration against the models for **(a)** daytime and **(b)** nighttime averaged cases.

Since in the global inversions usually afternoon CO_2 concentration data is used it is important to check how realistically the models used here simulate this kind of data. We analyzed CO_2 concentration time series averaged for daytime between 12:00 UTC to 17:00 UTC, which characterize the well-mixed hours for the region. Figure 6a demonstrates a comparison between all the models and the observation for the averaged concentration time during the well-mixed hours within one month period. The related statistics for the comparison are given in Table 2, indicating increasing correlation with increasing horizontal resolution. According to Table 2, the LMDZ model generally represents day-to-day variability of the afternoon averaged concentrations, while TM3 shows lower performance, especially in magnitude due to the above mentioned negative bias. The mean bias in LMDZ is larger than in WRF-VPRM. Only the root mean square errors are high in both models and even slightly bigger in WRF-VPRM. This can be explained by larger variability in the high-resolution model which leads to more scattering of the model predicted CO_2 fields (Fig. 3c). WRF-VPRM and LMDZ show quite good agreement against the observation until 27 May. On the following days we see a remarkable mismatch in the global models. On 30 May the observation showed the highest CO_2 signal during this period. Both LMDZ and TM3 underestimate this signal. However, WRF-VPRM captures this highest signal with some overestimation.

Focusing on night-time concentration (05:00–07:00 UTC, representing the later part of the night), WRF-VPRM agrees much better with the observations as compared to global models (Fig. 6b). From Fig. 6b and Table 2 it can be seen that generally the correlation between the models and the observation is slightly higher during night than during day; usually all models predict an early morning maximum in CO_2 concentrations due to release of CO_2 into nocturnal boundary layers. But the global models show significant deviation from the observation for the nighttime data. This discrepancy is caused by a poor simulation of nighttime vertical mixing. The correlation coefficients for both daytime and nighttime averaged CO_2 concentrations are significantly better in the high-resolution model. It is worth noting that WRF-VPRM can capture the phasing of the observed signal quite well, while there is some bias in amplitude, but much smaller than in the global models. This fact indicates that also for a mesoscale model such as WRF it is difficult to parameterize the nocturnal stable boundary layer, which is an active area of research in meteorology (Steeneveld, 2007).

5 Conclusions

We have used the high-resolution coupled atmosphere-biosphere model WRF-VPRM in order to interpret CO_2 concentration time series observed from a tower at the coastal station near Biscarosse during the CERES campaign in 2005. The station is strongly influenced by mesoscale flows. Sea-land breeze and its combination with local CO_2 fluxes can lead to a significant "contamination" of the observation signal, such that the time series is problematic to use quantitatively in coarse models. These errors come also from the poor simulation of vertical mixing during night and day over land. Similarly these kinds of errors are typical for stations located on complex terrain such as mountains.

Simulated CO_2 from two global models used in CO_2 inversions, TM3 and LMDZ, with different spatial resolutions, were compared with tower observations as well as with high-resolution simulation results from the coupled atmosphere-biosphere model WRF-VPRM. The results have shown that only WRF-VPRM is able to simulate the observed diurnal variability. The simulations also confirmed that recirculation of nighttime respired CO_2 requires modeling the covariance of mesoscale circulation and biospheric fluxes. Thus when our models are not able to simulate nighttime CO_2, then this may imply the "repeated bias" in daytime simulations due to recirculation with sea-breeze effect or in some cases frontal passage. One may conclude from such situations that even averaging CO_2 measurements over periods with a well-mixed boundary layer cannot prevent a contamination from recirculated continental respiration signals; consequently large representation errors in inversions when using such data are expected.

The work clearly demonstrates that an appropriate representation of synoptic variations and mesoscale effects can substantially improve representation of hourly CO_2. Undoubtedly a part of the differences between the models are caused by differences in the parameterizations, especially within the PBL schemes. WRF can be run with a different choice of PBL schemes, which in future studies should be used to investigate their impact and to validate these schemes using WRF-VPRM in comparison to CO_2 observations as a passive tracer.

Although we used fluxes from the simple diagnostic VPRM model that were not optimized against concentration measurements, the WRF-VPRM model is able to capture much more variability in the tower measured CO_2 time series. This indicates the importance of capturing the transport and mixing processes at high resolution and the spatiotemporal variability of biospheric fluxes that VPRM can represent. The high-resolution representation of the spatial heterogeneity in CO_2 fluxes especially in the near field is very important for properly simulating CO_2 distribution (Gerbig et al., 2009). In addition, a proper representation of the covariance between meteorology and biospheric CO_2 flux is necessary to capture rectifier effects (both, the normal rectification effect as well as the 3-D rectification effect) in order to avoid bias errors (Ahmadov et al., 2007).

This paper shows the potential of using WRF-VPRM in the context of inverse modeling in order to utilize high-frequency CO_2 concentration data. This is likely to improve inversion accuracy, and could extend the inverse modeling to "difficult sites" not used in current inversions. Running WRF-VPRM in very high resolution at global scale is computationally expensive, and needs to be used efficiently together with global inversion models. The run time of WRF-VPRM for one day on the 2 km grid is about 2–3 h on an Opteron cluster using 8 nodes (4 processors per node).

It is feasible to setup small domains around some measurement stations and to run a mesoscale model such as WRF-VPRM for these domains in high spatial resolution depending on the region and topography. Regional scale inversions can be done using the STILT-VPRM modeling framework (Matross et al., 2006), which can be driven by WRF generated transport fields. Rödenbeck et al. (2009) showed that such nested inversions within global models are feasible, even with completely different transport representations for global and regional scales. Moreover forward modeling of CO_2 transport by WRF-VPRM for some sites is an essential to validate the model, and provides a better understanding of near-field influence on measurements at continental sites and consequently on regional flux estimates (Lauvaux et al., 2008). Using such flexible modeling tools as WRF would allow us to test different physics and dynamics options in order to improve modeling capabilities for a given region.

The agreement of nighttime simulated CO_2 with observations suggests that it should be feasible to also use the nighttime observations in the inversions, providing important information on the partitioning of biosphere-atmosphere exchange between respiration and photosynthesis. Lauvaux et al. (2008) has found that improving the transport simulation for nocturnal CO_2 concentrations at tower sites would lead to large error reduction in CO_2 inversions. Although proper simulation of the stable boundary layers remains difficult even in advanced mesoscale models such as WRF, there is hope that within the large community involved in WRF model development (http://wrf-model.org) there will be substantially improvements in its capabilities to simulate mixing in nighttime cases. Inversion studies would be able to constrain respiration fluxes at regional scales using the numerous continuous CO_2 monitoring sites by involving nighttime data from continental sites in addition to the daytime data.

Because of its great flexibility, WRF-VPRM can serve to bridge the gap between the measurements and inversion models in almost all regions of the globe including complex terrain areas. The fast growing global greenhouse gas monitoring network makes this tool attractive.

Acknowledgements. The authors are grateful to all the CERES community for providing the measurement results. We thank the technical teams from RAMCES and DAPNIA/SIS for the maintenance of the CARIBOU analyzer. We acknowledge G. Boenisch from MPI BGC for the help in getting the meteorological data from the NOAA database. We thank S. Schott for her support in the layout. The authors appreciate the valuable comments of the two reviewers R. Law and A. Meesters.

Edited by: H. Dolman

The service charges for this open access publication
have been covered by the Max Planck Society.

References

Ahmadov, R., Gerbig, C., Kretschmer, R., et al.: Mesoscale covariance of transport and CO_2 fluxes: Evidence from observations and simulations using the WRF-VPRM coupled atmosphere-biosphere model, J. Geophys. Res.-Atmos., 112(D22), D22107, doi:10.1029/2007JD008552, 2007.

Bakwin, P. S., Tans, P. P., Zhao, C. L., Ussler III, W., and Quesnell, E.: Measurements of carbon dioxide on a very tall tower, Tellus B, 47(5), 535–549, 1995.

Denning, A. S., Nicholls, M., Prihodko, L., et al.: Simulated variations in atmospheric CO_2 over a Wisconsin forest using a coupled ecosystem-atmosphere model, Glob. Change Biol., 9(9), 1241–1250, 2003.

Dolman, A. J., Noilhan, J., Durand, P., et al.: The CarboEurope regional experiment strategy, B. Am. Meteorol. Soc., 87(10), 1367–1379, 2006.

Geels, C., Gloor, M., Ciais, P., Bousquet, P., Peylin, P., Vermeulen, A. T., Dargaville, R., Aalto, T., Brandt, J., Christensen, J. H., Frohn, L. M., Haszpra, L., Karstens, U., Ródenbeck, C., Ramonet, M., Carboni, G., and Santaguida, R.: Comparing atmospheric transport models for future regional inversions over Europe – Part 1: Mapping the atmospheric CO_2 signals, Atmos. Chem. Phys., 7, 3461–3479, 2007, http://www.atmos-chem-phys.net/7/3461/2007/.

Gerbig, C., Dolman, A. J., and Heimann, M.: On observational and modelling strategies targeted at regional carbon exchange over continents, Biogeosciences Discuss., 6, 1317–1343, 2009, http://www.biogeosciences-discuss.net/6/1317/2009/.

Gerbig, C., Körner, S., and Lin, J. C.: Vertical mixing in atmospheric tracer transport models: error characterization and propagation, Atmos. Chem. Phys., 8, 591–602, 2008, http://www.atmos-chem-phys.net/8/591/2008/.

Gurney, K. R., Law, R. M., Denning, A. S., et al.: Towards robust regional estimates of CO_2 sources and sinks using atmospheric transport models, Nature, 415, 6872, 626–630, 2002.

Gurney, K. R., Law, R. M., Denning, A. S., et al.: Transcom 3 inversion intercomparison: Model mean results for the estimation of seasonal carbon sources and sinks, Global Biogeochem. Cy., 18(1), GB1010, doi:10.1029/2003GB002111, 2004.

Hansen, J., Sato, M., Ruedy, R., Kharecha, P., Lacis, A., Miller, R., Nazarenko, L., Lo, K., Schmidt, G. A., Russell, G., Aleinov, I., Bauer, S., Baum, E., Cairns, B., Canuto, V., Chandler, M., Cheng, Y., Cohen, A., Del Genio, A., Faluvegi, G., Fleming, E., Friend, A., Hall, T., Jackman, C., Jonas, J., Kelley, M., Kiang, N. Y., Koch, D., Labow, G., Lerner, J., Menon, S., Novakov, T., Oinas, V., Perlwitz, Ja., Perlwitz, Ju., Rind, D., Romanou, A., Schmunk, R., Shindell, D., Stone, P., Sun, S., Streets, D., Tausnev, N., Thresher, D., Unger, N., Yao, M., and Zhang, S.: Dangerous human-made interference with climate: a GISS modelE study, Atmos. Chem. Phys., 7, 2287–2312, 2007, http://www.atmos-chem-phys.net/7/2287/2007/.

Heimann, M. and Reichstein, M.: Terrestrial ecosystem carbon dynamics and climate feedbacks, Nature, 451, 7176, 289–292, 2008.

Hourdin, F. and Armengaud, A.: The use of finite-volume methods for atmospheric advection of trace species. Part I: Test of various formulations in a general circulation model, Mon. Weather Rev., 127(5), 822–837, 1999.

Jung, M., Henkel, K., Herold, M., and Churkina, G.: Exploiting synergies of global land cover products for carbon cycle modeling, Remote Sens. Environ., 101(4), 534–553, 2006.

Lauvaux, T., Uliasz, M., Sarrat, C., Chevallier, F., Bousquet, P., Lac, C., Davis, K. J., Ciais, P., Denning, A. S., and Rayner, P. J.: Mesoscale inversion: first results from the CERES campaign with synthetic data, Atmos. Chem. Phys., 8, 3459–3471, 2008, http://www.atmos-chem-phys.net/8/3459/2008/.

Law, R. M., Peters, W., Rodenbeck, C., et al.: TransCom model simulations of hourly atmospheric CO2: Experimental overview and diurnal cycle results for 2002, Global Biogeochem. Cy., 22(3), GB3009, doi:10.1029/2007GB003050, 2008.

Law, R. M., Rayner, P. J., Steele, L. P., and Enting, I. G.: Using high temporal frequency data for CO_2 inversions, Global Biogeochem. Cy., 16(4), 1053, doi:10.1029/2001GB001593, 2002.

Lin, J. C. and Gerbig, C.: Accounting for the effect of transport errors on tracer inversions, Geophys. Res. Lett., 32(1), L01802, doi:10.1029/2004GL021127, 2005.

Macatangay, R., Warneke, T., Gerbig, C., Körner, S., Ahmadov, R., Heimann, M., and Notholt, J.: A framework for comparing remotely sensed and in-situ CO_2 concentrations, Atmos. Chem. Phys., 8, 2555–2568, 2008, http://www.atmos-chem-phys.net/8/2555/2008/.

Mahadevan, P., Wofsy, S. C., Matross, D. M., et al.: A satellite-based biosphere parameterization for net ecosystem CO_2 exchange: Vegetation Photosynthesis and Respiration Model (VPRM), Global Biogeochem. Cy., 22, GB2005, doi:10.1029/2006GB002735, 2008.

Matross, D. M., Andrews, A., Pathmathevan, M., et al.: Estimating regional carbon exchange in New England and Quebec by combining atmospheric, ground-based and satellite data, Tellus B, 58(5), 344–358, 2006.

Pérez-Landa, G., Ciais, P., Gangoiti, G., Palau, J. L., Carrara, A., Gioli, B., Miglietta, F., Schumacher, M., Millán, M. M., and Sanz, M. J.: Mesoscale circulations over complex terrain in the Valencia coastal region, Spain – Part 2: Modeling CO_2 transport using idealized surface fluxes, Atmos. Chem. Phys., 7, 1851–1868, 2007, http://www.atmos-chem-phys.net/7/1851/2007/.

Peylin, P., Rayner, P. J., Bousquet, P., Carouge, C., Hourdin, F., Heinrich, P., Ciais, P., and AEROCARB contributors: Daily CO_2 flux estimates over Europe from continuous atmospheric measurements: 1, inverse methodology, Atmos. Chem. Phys., 5, 3173–3186, 2005, http://www.atmos-chem-phys.net/5/3173/2005/.

Riley, W. J., Randerson, J. T., Foster, P. N., and Lueker, T. J.: Influence of terrestrial ecosystems and topography on coastal CO_2 measurements: A case study at Trinidad Head, California. J. Geophys. Res.-Biogeosciences, 110(G1), G01005, doi:10.1029/2004JG000007, 2005.

Rödenbeck, C., Gerbig, C., Trusilova, K., and Heimann, M.: A two-step scheme for high-resolution regional atmospheric trace gas inversions based on independent models, Atmos. Chem. Phys. Discuss., 9, 1727–1756, 2009, http://www.atmos-chem-phys-discuss.net/9/1727/2009/.

Rödenbeck, C., Houweling, S., Gloor, M., and Heimann, M.: CO_2 flux history 1982–2001 inferred from atmospheric data using a global inversion of atmospheric transport, Atmos. Chem. Phys., 3, 1919–1964, 2003, http://www.atmos-chem-phys.net/3/1919/2003/.

Sarrat, C., Noilhan, J., Dolman, A. J., Gerbig, C., Ahmadov, R., Tolk, L. F., Meesters, A. G. C. A., Hutjes, R. W. A., Ter Maat, H. W., Pérez-Landa, G., and Donier, S.: Atmospheric CO_2 modeling at the regional scale: an intercomparison of 5 meso-scale atmospheric models, Biogeosciences, 4, 1115–1126, 2007, http://www.biogeosciences.net/4/1115/2007/.

Sellers, P. J., Los, S. O., Tucker, C. J., et al.: A revised land surface parameterization (SiB2) for atmospheric GCMs .2. The generation of global fields of terrestrial biophysical parameters from satellite data, J. Climate, 9(4), 706–737, 1996.

Steeneveld, G.: Understanding and Prediction of Stable Atmospheric Boundary Layers over Land, PhD thesis, 2007.

Tans, P. P., Fung, I. Y., and Takahashi, T.: Observational constraints on the global atmospheric CO_2 budget, Science, 247, 4949, 1431–1438, 1990.

Trusilova, K. and Churkina, G.: The Terrestrial Ecosystem Model GBIOME-BGCv1, Technical Reports – Max-Planck-Institut für Biogeochemie (14), 61 pp., 2008.

van der Molen, M. K. and Dolman, A. J.: Regional carbon fluxes and the effect of topography on the variability of atmospheric CO_2, J. Geophys. Res.-Atmos., 112(D1), D01104, doi:10.1029/2006JD007649, 2007.

Wang, J.-W., Denning, A. S., Lu, L. X., et al.: Observations and simulations of synoptic, regional, and local variations in atmospheric CO_2, J. Geophys. Res.-Atmos., 112(D4), D04108, doi:10.1029/2006JD007410, 2007.